

PACS numbers: 42.62.Be; 07.57.Pt; 87.57. –s
DOI: 10.1070/QE2008v038n07ABEH013851

Terahertz time-domain spectroscopy of biological tissues

M.M. Nazarov, A.P. Shkurinov, E.A. Kuleshov, V.V. Tuchin

Abstract. **Terahertz absorption spectra and dispersion of biologically important substances such as sugar, water, hemoglobin, lipids and tissues are studied. The characteristic absorption lines in the frequency range of a terahertz spectrometer (0.1 – 3.5 THz) are found. The refraction indices and absorption coefficients of human tooth enamel and dentine are measured. The method of terahertz phase reflection spectroscopy is developed for strongly absorbing substances. Simple and reliable methods of time-resolved terahertz spectroscopy are developed.**

Keywords: *terahertz spectroscopy, tissues, biomolecules.*

1. Introduction

The terahertz frequency range lying between the IR and microwave ranges (1 THz → 1 ps → 300 μm → 33 cm^{-1} → 4.1 meV → 47.6 K) is at present the last poorly studied frequency range in the entire scale of electromagnetic waves from radio-frequency to X-ray range. Efficient generators and low-noise detectors for this frequency range became available only in the last two decades, mainly due to the development of ultrashort-pulse lasers. Terahertz radiation is perspective for spectroscopic [1] and medicical applications [2 – 5]. It is known that biological tissues have small dispersion and large absorption in the terahertz range [6]. Many vibrational transitions in simple biomolecules are located in this range. In addition, inhomogeneities smaller than 0.1 mm producing strong scattering in the visible and near-IR spectral regions do not cause considerable scattering in the terahertz range. The use of ultrashort pulses allows one to study a broad frequency range in one measurement with a high time resolution.

M.M. Nazarov, A.P. Shkurinov, E.A.Kuleshov Department of Physics, M.V. Lomonosov Moscow State University, Vorob'evy gory, 119992 Moscow, Russia; e-mail: maxim@lasmed.phys.msu.ru;
V.V. Tuchin Department of Optics and Biomedical Physics, Research and Educational Institute of Optics and Biophotonics, N.G. Chernyshevskii Saratov State University, ul. Astrakhanskaya 83, 410012 Saratov, Russia; Institute of Problems of Precise Mechanics and Control, Russian Academy of Sciences, ul. Rabochaya 24, 410028 Saratov, Russia; e-mail: tuchin@sgu.ru

Received 20 March 2008
Kvantovaya Elektronika **38** (7) 647 – 654 (2008)
Translated by M.M. Nazarov

The aim of our work is to develop the methods for studying biological tissues in the terahertz frequency range providing the detection and visualisation of metabolic and pathological processes in tissues. The determination of absorption lines and transparency windows inherent in tissues and molecules involved in metabolic processes is necessary for the development of a terahertz spectrometer with the maximal sensitivity and selectivity to changes occurring in biomolecules. In addition, such information on biological tissues will allow one to detect the presence and changes in substances with the characteristic spectrum of the complex refractive index. These studies are important for the development of a terahertz tomograph with a high sensitivity to changes in the concentration of metabolites, which can provide accurate determination of the boundaries of pathologic process based on information about the complex refraction index of biological tissues obtained with a high spatial resolution.

2. Measurement principles

We used several known methods for generating terahertz pulses, in which short laser pulses are converted to the terahertz range in a photoconductive antenna, a semiconductor or a nonlinear crystal. In the first two cases, radiation is generated due to the creation of the transient electron – hole photoconduction in a semiconductor irradiated by light pulses [7] and due to a photocurrent pulse caused by the action of the external or internal electric field. In the latter case, a difference frequency is generated in a nonlinear crystal [8] (optical rectification).

Terahertz pulses (THPs) are detected in a similar photoconductive antenna or by using the electrooptical effect in a nonlinear crystal [8]. The THP field induces birefringence in a crystal, the polarisation of a probe laser pulse changing proportionally to the THP field amplitude at a given instant. In the experiment, the difference of powers of orthogonal polarisation components of the probe laser pulse or a current induced in the antenna depending on the time delay between terahertz and optical pulses is measured. The detector sensitivity and the THP generator efficiency were determined by phase matching parameters, the nonlinear susceptibility, the crystal length and the laser pulse duration. When semiconductor devices were replaced by nonlinear-optical devices, the frequency range of a spectrometer (0.5 ± 0.45 THz) shifted to the high-frequency region (2 ± 1.5 THz).

A time-domain terahertz spectrometer scheme used in our study (Fig. 1) is described in detail in [9]. The THP

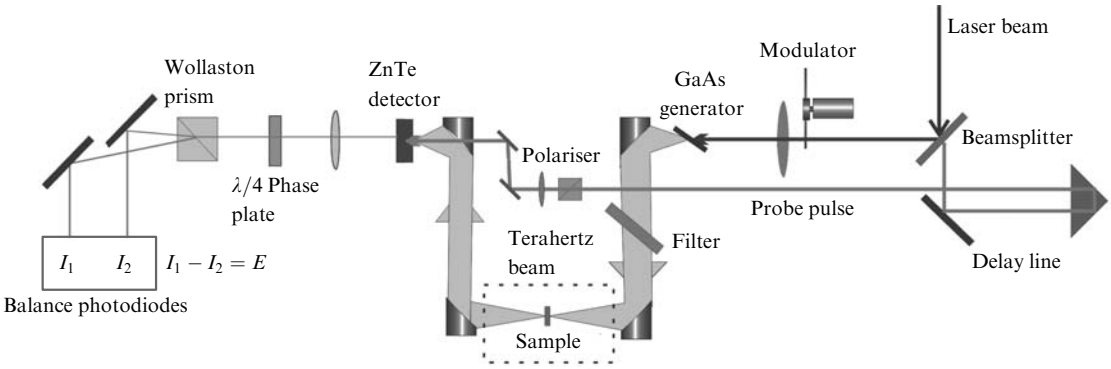

Figure 1. Scheme of a time-domain terahertz spectrometer.

detector and generator types were chosen depending on the absorption in a sample and the frequency range of interest [10]. For example, measurements in the range from 2.5 to 3.5 THz not easily accessible for time-domain spectroscopy were performed by using 90-fs laser pulses at 790 nm. Terahertz pulses were generated by a low-temperature grown GaAs semiconductor surface; an electrooptical detector was made of a 0.3-mm-thick $\langle 110 \rangle$ ZnTe crystal. By using the Fourier transform of the temporal THP profile, we calculated the complex spectrum containing information on the refractive index and absorption coefficient of the medium [11].

In most of experiments we used time sampling containing 1024 points of 50-ps duration, with the signal acquisition time of 300 ms at each point. This allowed us to perform measurements with the signal-to-noise ratio (SNR) more than 10^2 in the spectral range from 0.3 to 2.5 THz with a spectral resolution of 10 GHz. Laser and terahertz pulses had a repetition period of 12 ns, the THP energy probing a biological tissue being $\sim 10^{-13}$ J. Such a low pulse energy should not damage the tissue. Even in the case of a resonance absorption, only a small fraction of pulse spectral components is absorbed in a sample.

Methods for measuring the absorption coefficient and refractive index. A specific feature of time-domain terahertz spectroscopy is the possibility of direct measurements of the electromagnetic field strength and direction, which gives information on the amplitude and phase and allows the calculation of the refractive index, absorption coefficient and dispersion of the medium under study.

To calculate optical properties of a tissue it is necessary to reconstruct optical parameters from the measured transmission spectra $T(\omega)$ [12]. From the experiment and subsequent Fourier transform of the temporal profiles of pulses we obtain the incident THP amplitude $[E_{\mathrm{ref}}(\omega)]$ and the amplitude $[E_{\mathrm{sam}}(\omega)]$ of the transmitted field and then calculate the transmission coefficient of a sample:

$$T(\omega) = \frac{E_{\mathrm{sam}}}{E_{\mathrm{ref}}} = T_0(\omega)\mathrm{FP}(\omega)\mathrm{RL}(\omega), \tag{1}$$

where

$$T_0(\omega) = \exp\left[-\mathrm{i}(n_{\mathrm{sam}} - n_{\mathrm{air}})\frac{d\omega}{c}\right] \tag{2}$$

contains the basic information on the medium through which THP has passed (the absorption coefficient and refractive index of the sample);

$$\mathrm{RL}(\omega) = \frac{4n_{\mathrm{sam}}n_{\mathrm{air}}}{(n_{\mathrm{sam}} + n_{\mathrm{air}})^2} = 1 - R^2(\omega) \tag{3}$$

describes reflection losses from sample boundaries;

$$\mathrm{FP}(\omega) = \left[1 - R^2(\omega)\exp\left(-\mathrm{i}2n_{\mathrm{sam}}\frac{d\omega}{c}\right)\right]^{-1} \tag{4}$$

describes multiply reflected pulses in a parallel plate – Fabry–Perot modes; $n(\omega) = n'(\omega) - \mathrm{i}n''(\omega)$ are complex refractive indices for the corresponding medium; $n''(\omega) = \alpha(\omega)c/\omega$ is absorption taken into account in the imaginary part of n; $\omega = 2\pi f$ is the cyclical frequency; $R(\omega) = (n_{\mathrm{sam}} - n_{\mathrm{air}})/(n_{\mathrm{sam}} + n_{\mathrm{air}})$ is the complex reflection coefficient; c is the speed of light; $n_{\mathrm{air}} \approx 1$; and d is the sample thickness. Note that we use the absorption coefficient for the field, while in other methods the power absorption coefficient, which is twice larger, is commonly used.

Equation (1) cannot be solved analytically, but for most cases the approximate solution is valid. By assuming that $\mathrm{RL}(\omega) \approx \mathrm{const}$, and $\mathrm{FP}(\omega) \approx 1$, we obtain:

$$\alpha(\omega) = \frac{-\ln|T(\omega)|}{d} + \frac{\ln(1 - R_{\mathrm{av}}^2)}{d}, \tag{5}$$

where $R_{\mathrm{av}} = (n_{\mathrm{av}} - 1)/(n_{\mathrm{av}} + 1)$ is the reflection coefficient, for the real part of the refractive index of the sample, averaged over the frequency range of measurements. The averaged refractive index n_{av} can be easily determined in the time domain from the delay Δt of a pulse propagating through the sample

$$n_{\mathrm{av}} = 1 + \Delta t\,\frac{c}{d}. \tag{6}$$

The frequency dependence of the refractive index has the form:

$$n'(\omega) = -\arg\{T(\omega)\}\frac{c}{\omega d} + 1. \tag{7}$$

In a rigorous case it is necessary to take into account multiple reflections from the sample edges – Fabry–Perot modes [9]; this is important in the case of a large refractive index and thin samples – in our case, in the spectral measurements of tooth slices and pressed saccharide pellets.

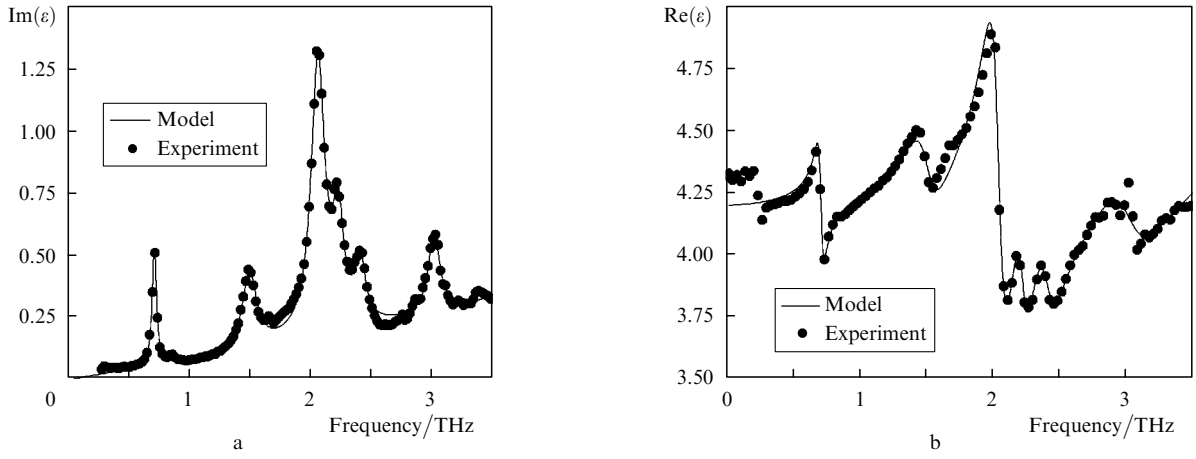

Figure 2. Spectra of the real (a) and imaginary (b) parts of the permittivity of L-cystine.

Model spectra. To analyse modifications observed in tissues, characteristic absorption lines of the substances contained in tissues were described by a simple model. The permittivity is described by the sum of Lorentz oscillators [13]:

$$\varepsilon(\omega) = \varepsilon_0 + \sum_j \frac{S_j \omega_j^2}{(\omega_j^2 - \omega^2) - \mathrm{i}\Gamma_j \omega}, \tag{8}$$

where ω_j, Γ_j, S_j are eigenfrequencies, dumping factors and oscillator strengths, respectively; ε_0 is the low-frequency permittivity; j is the number of a resonance in the selected frequency range. Figure 2 presents the spectra of the real and imaginary parts of the permittivity measured for L-cystine polypeptide [1, 14] and the corresponding model curves.

The permittivity ε is related to the complex refractive index as $\varepsilon = n^2$, and the absorption coefficient and refractive index can be measured experimentally by using (5) and (7) and then constants can be selected for ε in (8). The applicability of the model for various substances was verified by using spectral data obtained for ε and n in [14, 15].

Terahertz reflection spectroscopy. Transmission spectroscopy is not suitable for a number of objects because of their large absorption (for example water containing tissues) or because of large sizes (*in vivo* measurements). In this case, reflection spectroscopy is more convenient. The complex reflection coefficient

$$\tilde{R}_\mathrm{p}(\omega) = \frac{n^2(\omega)\cos(\theta) - \left[n^2(\omega) - \sin^2(\theta)\right]^{1/2}}{n^2(\omega)\cos(\theta) + \left[n^2(\omega) - \sin^2(\theta)\right]^{1/2}} \tag{9}$$

measured in these experiments is characterised by amplitude R and phase φ ($\tilde{R}_\mathrm{p} = R\mathrm{e}^{\mathrm{i}\varphi}$), where the subscript p denotes radiation polarisation in the plane of incidence, θ is the angle of beam incidence with respect to the normal. We used here the Fresnel formula taking into account the complex part of the refractive index. A comparison of the model reflection coefficients for different angles of incidence θ showed that the most sensitive to the presence of absorption lines is p-polarisation, especially, its phase characteristic. We selected the angle of incidence $\theta_0 = \arctan(n') - 5^\circ$ corresponding to the high sensitivity of the method to characteristic absorption lines. When θ_0 is close

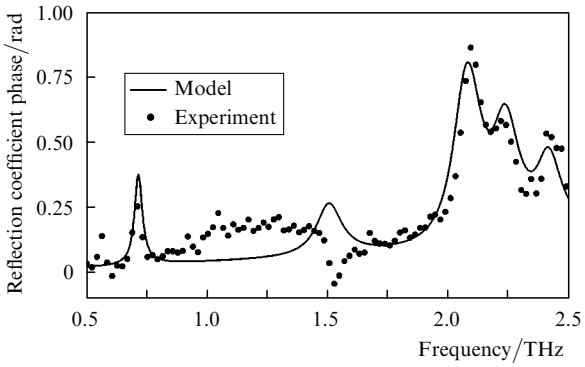

Figure 3. Reflection coefficient phase spectrum of L-cystine at a angle of incidence of 63°.

to the Brewster angle $\theta_\mathrm{Br} = \arctan(n')$, resonance lines are best pronounced in the reflection spectrum; however, at $\theta_0 = \theta_\mathrm{Br}$ the amplitude R tends to zero, which complicates the experiment. We measured and simulated the reflection spectrum of L-cystine (Fig. 3). Note that the phase of the reflection spectrum repeats in fact the shape of the imaging part of the permittivity (Fig. 2).

Two questions arise that are principal for investigations of biological tissues and concern the probing depth and layered structure of media. The measurement method proposed above gives only information on the interface (the effective thickness at which the reflected signal is formed is tens of microns). If layered media are studied, for the layer thickness ~ 100 μm and more, pulses reflected from different surfaces can be separated in time. Then, we can apply expression (9) for each layer with its own reflection coefficient and bulk parameters of the layer between surfaces through which radiation propagates twice. In the visible range this method is developed, for example, for a three-layer skin model [16], which can be adapted to the terahertz range.

Total internal reflection. To study soft tissues or aqueous solutions, the total internal reflection (TIR) spectroscopy is more convenient. In this case, it is possible to control the penetration depth of the field in matter. We calculated and manufactured a silicon Doe prism with the 1.5×2 cm base and the apex angle of 90°. The refractive index of silicon in the terahertz range is 3.42, while dispersion and absorption are virtually absent. This prism placed in a collimated

terahertz beam does not change its direction. As the reference signal we used reflection from the clean prism base, the measurement signal was obtained when a substance under study was pressed against the prism base (or liquid under study was poured on the base). We performed TIR test experiments with water and aqueous solutions and the hand wrist skin (*in vivo*).

The main advantage of the TIR method over reflection spectroscopy is the simplicity of measuring the reference spectrum (without substance); in addition, the reflection coefficient amplitude is close to unity. The main difficulty of the TIR method is to provide the optical contact in studies of hard samples. The simulation of a three-layer system (prism – air – substance) by using experimental parameters showed that the presence of the air layer of only 10 μm in thickness is already critical. In the case of liquid samples, the optical contact is good and this problem is absent. Fresnel formulas describing the reflection spectrum are also valid for TIR if the refractive index of the prism is taken into account and n is replaced by n/n_{pr} in (9). On passing from measurements of the reflection spectrum of an open surface to a scheme with a prism, the spectra of the phase and amplitude of the reflection coefficient change qualitatively.

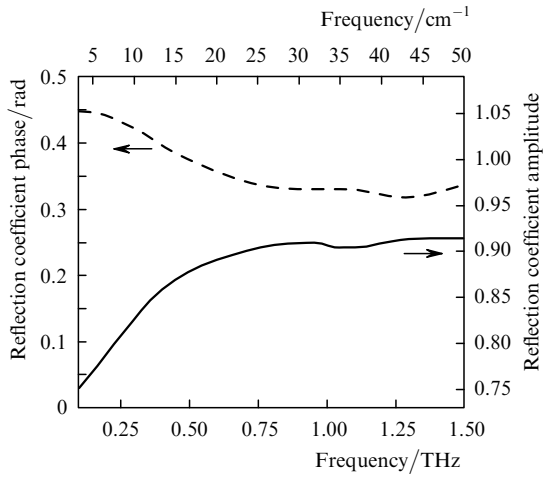

Figure 4. Reflection coefficient amplitude and phase spectra of the hand skin upon TIR.

The scheme with a prism is more convenient for studying soft tissues because pressing against the prism base provides the flat smooth interface of a sample. We measured the reflection spectrum of the wrist skin (32 years old white man, palm near the thumb base) (Fig. 4).

Because the high sensitivity of the TIR method is provided in surface tissue layers up to 10 μm, the skin was probed only by the depth of the corneous layer in which the water content is minimal (15 %). This layer consists mainly of proteins (70 %) and lipids (15 %) [17], and therefore the reflection spectrum of skin considerably differs from that of water.

By using the methods described above, we measured the terahertz absorption and refraction spectra of some saccharides and other biologically important substances.

Absorption and refraction in liquids. The most important substance contained in living systems is liquid water, its average content in biological tissues achieving 75 % [18]. Liquid water strongly absorbs radiation in the terahertz range. A 200-μm-thick water layer attenuates the radiation field at a frequency of 1 THz by an order of magnitude, while a 1-mm-thick water in layer is almost opaque in the terahertz range. The permittivity of water is known [19] and can be described by the two-component Debye model with the Lorentz term [4]:

$$\varepsilon(\omega) = \varepsilon_\infty + \frac{\varepsilon_{\mathrm{s}} - \varepsilon_1}{1 + \mathrm{i}\omega\tau_{\mathrm{D}}} + \frac{\varepsilon_1 - \varepsilon_\infty}{1 + \mathrm{i}\omega\tau_2} + \frac{A}{\omega_0^2 - \omega^2 + \mathrm{i}\omega\gamma}, \quad (10)$$

where $\tau_{\mathrm{D}} = 9.36$ ps and $\tau_2 = 0.3$ ps are the response times of the first and second Debye terms; $\varepsilon_\infty = 2.5$ is the high-frequency permittivity; $\varepsilon_{\mathrm{s}} = 80.2$ and $\varepsilon_1 = 5.3$ are contributions to the low-frequency permittivity from the first and second Debye terms; $A = 38(\mathrm{THz}/2\pi)^2$, $\omega_0 = 5.6$ THz$/2\pi$, and $\gamma = 5.9$ THz are the amplitude, frequency and linewidth of the Lorentz term, respectively. The reflection spectrum of liquid water calculated by (9) and (10) and the measured spectrum are presented in Fig. 5a. Note that the TIR method expands the spectral range of measurements from 1 THz [2] to 2.5 THz.

Many substances are contained in tissues in aqueous solutions. In principle they can be detected by the method of time-domain terahertz spectroscopy. The addition of solvable substances into water noticeably changes the TIR spectrum, which was demonstrated for the spectrum of

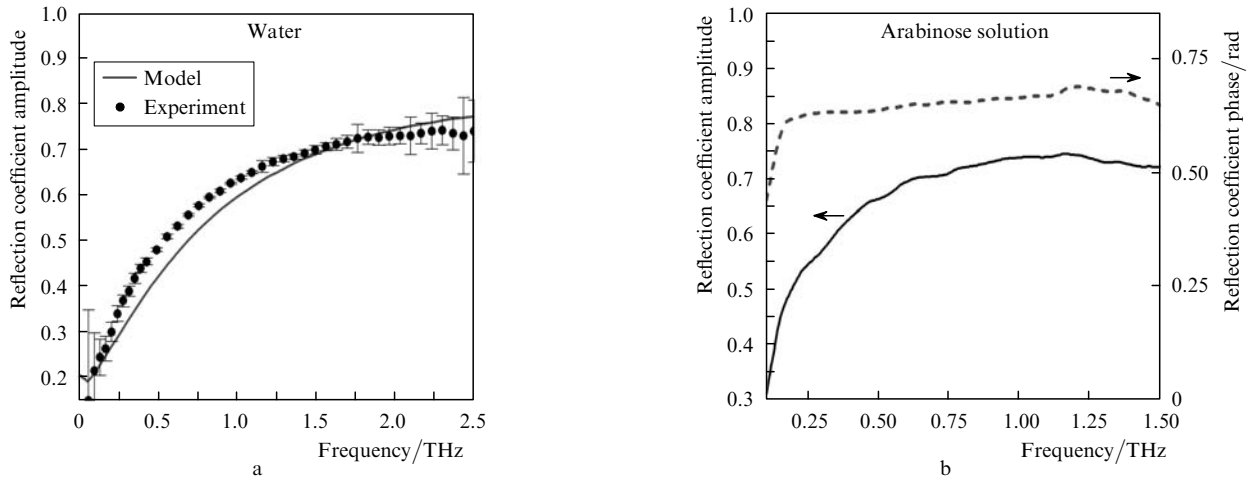

Figure 5. Reflection spectra of water (a) and the saturated water solution of arabinose (b).

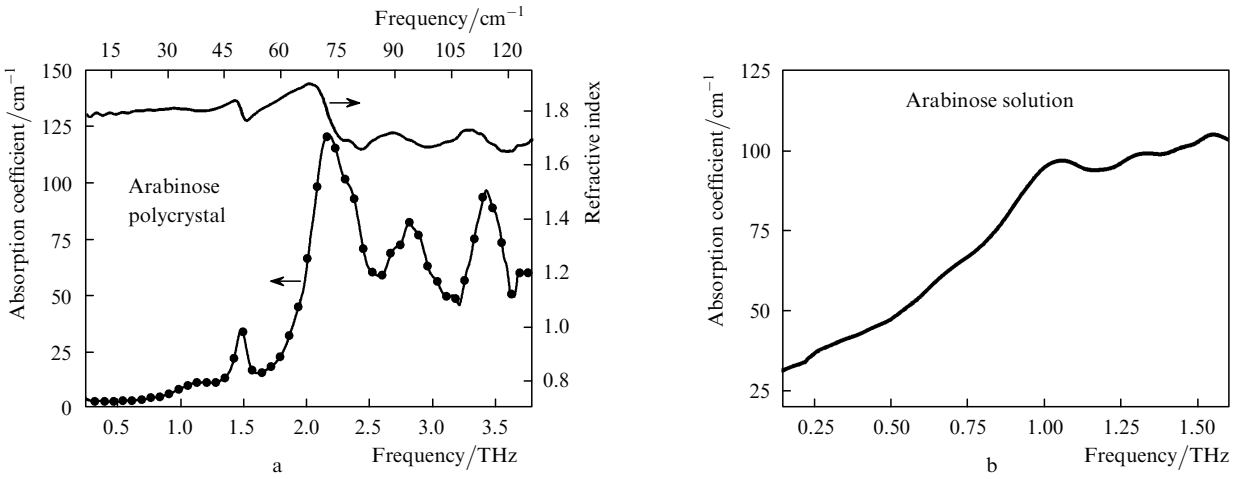

Figure 6. Absorption spectra of arabinose powder (a) and its saturated solution (b).

saturated arabinose solution (at 21 °C, the arabinose : water mass ratio 1 : 1) measured by using a scheme with a prism (Fig. 5b).

For comparison, the absorption spectra of dry arabinose (a 200-μm-thick pellet of diameter 5 mm pressed from powder at a pressure of 1 ton) and of its aqueous solution are presented in Fig. 6. The phonon absorption lines disappear in the solution and molecular vibrational lines strongly broaden and cannot be resolved. In our case, the reflection spectrum of arabinose at the high concentration differs from that of pure water (in the range from 0.5 to 1 THz).

The absorption spectra of other liquids [chicken fat at 21 °C and vegetable oils (sunflower and olive)] presented in Fig. 7 are almost the same in this spectral range. Note that fats have good transparency, weak dispersion and a peculiarity in the range from to 2 to 2.5 THz. This means that time-domain terahertz spectroscopy can be used to measure the thickness of fat layers (by the delay of THPs reflected from the first and second boundaries of layers).

Absorption in saccharides. The absorption spectra of several saccharides are presented in Fig. 8. Each saccharide has its own characteristic absorption lines. Note that terahertz spectroscopy is sensitive to the presence of bound water in molecules (glucose monohydrate and glucose have different absorption spectra).

Different saccharides exhibit both similar absorption lines (in the ranges 1.6 – 1.9 THz and 2.6 – 2.8 THz) and characteristic lines (Figs 8 and 6a). In the general case, the number of lines and nonresonance background absorption increase with increasing frequency. The lowest-frequency line can be treated as the characteristic line because its frequency depends on saccharide. It is equal to 0.54, 1.44, 1.48, 1.72, 1.82, and 1.83 THz for lactose, glucose monohydrate, arabinose, fructose, glucose, and saccharose, respectively. This means that it is possible to determine the relative content of different components in their mixture if their absorption spectra are known. One can see that the absorption spectrum of the glucose – L-cystine mixture (Fig. 9a) contains information on both components, although it is not the exact sum of the absorption spectra of individual components.

We made an attempt to detect the presence of glucose in hemoglobin (in a dried sample, Fig. 9b). However, absorption in hemoglobin was strong in the entire spectral range and had no specific spectral features [10], which did not allow us to detect the presence of glucose (12 % by mass) by its characteristic absorption lines.

Tissues. The study of biological tissues (Fig. 10) has shown that they have high and comparable absorption but their refractive indices are considerably different. The latter allows us to measure pulses reflected from different layers of

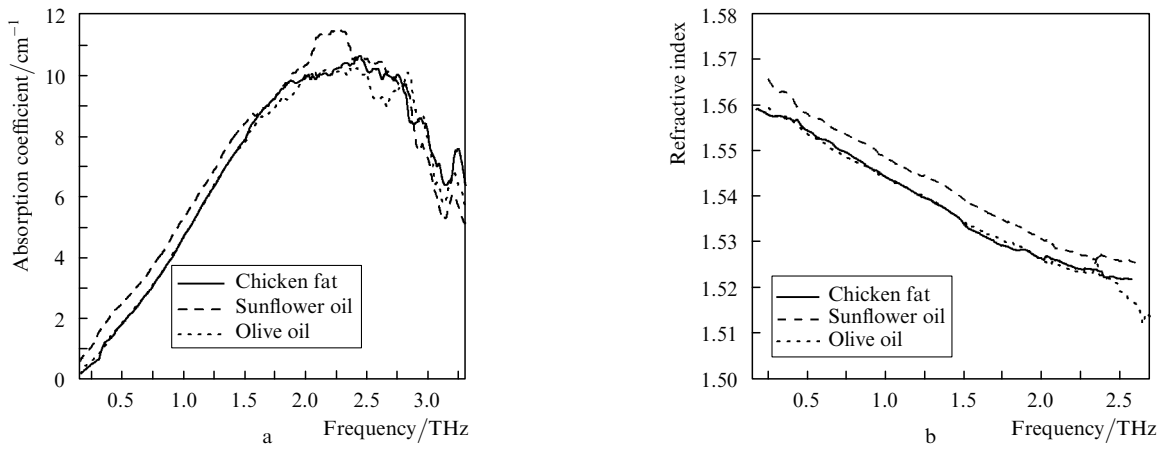

Figure 7. Absorption (a) and refraction (b) spectra of melted chicken fat and vegetable oils.

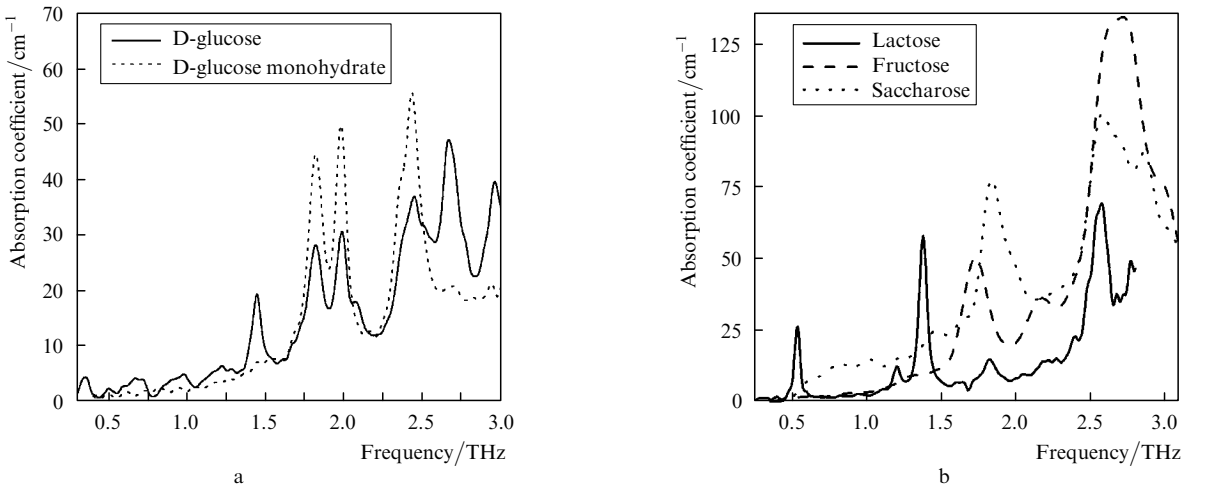

Figure 8. Absorption spectra of several types of saccharides.

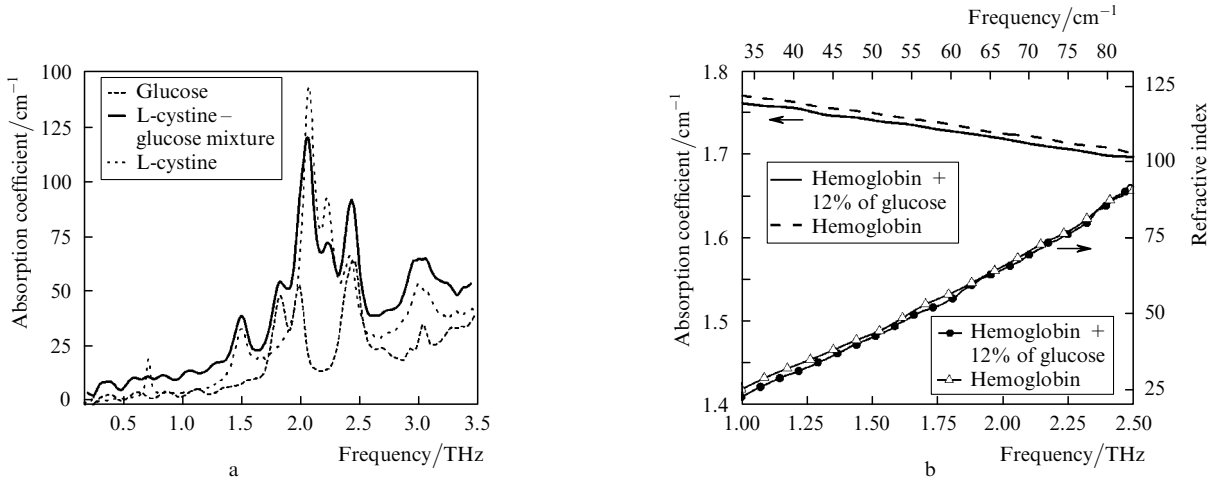

Figure 9. Terahertz absorption spectra of mixtures and pure substances (a) and the absorption of hemoglobin with glucose (b).

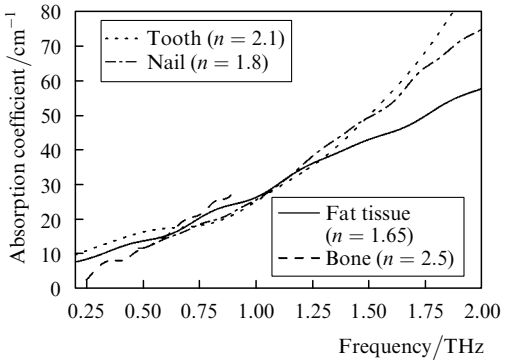

Figure 10. Absorption spectra of biological tissues (values of n are averaged).

the tissue if the signal-to-noise ratio in a time-domain terahertz spectrometer is significantly increased.

The absorption and refraction spectra of biological tissues have a similar shape. This is partly explained by the presence of water in them (the absorption spectrum of water has the same shape [4, 10, 20], but the absorption coefficient of water is several times higher). The absorption spectra of biological molecules have a similar shape (linear or quadratic increase in absorption and a decrease in the refractive index with frequency). The absence of characteristic lines in the spectra of 'dry' tissues can be explained by the overlap of many spectral lines in the high-frequency range. However, this question requires more detailed investigation.

3. Spectra of different tooth sites

Tooth tissues were studied by the method of time-domain terahertz spectroscopy in papers [4, 19]. At present more detailed information on these tissues is needed, including the monitoring of different types of dentine and obtaining more detailed spectral characteristics. Although the water content in dentine and enamel is small, it affects their optical properties, which was also demonstrated by other methods [21, 22]. The results of measurements presented here are important for the development of terahertz tooth tomography [19], in particular, for diagnostics of some diseases related to variations in the water content in tooth tissues, for drug diffusion and tooth liquor *in vivo* monitoring. The monitoring of pathological changes in tooth tissues requires the knowledge of the main optical

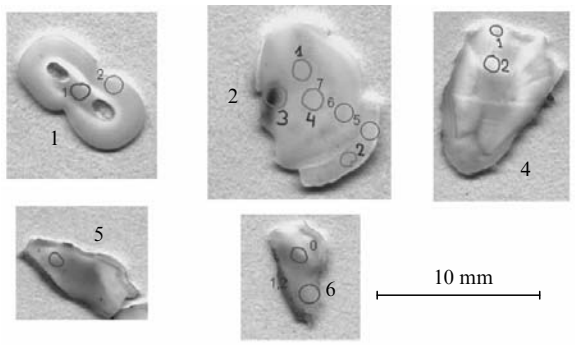

Figure 11. Tooth slice images with indicated sites for spectral measurements.

characteristics of various tooth tissues in the terahertz frequency range. We measured locally (the diameter of the measured site was ~ 1 mm) the transmission spectra of different tooth sites (Fig. 11), including dentine areas with different concentration and orientation of dentine tubules [22, 23].

The study revealed a considerable difference between the refraction indices of dentine and enamel. The absorption spectra of different samples without pathology coincided in fact with each other. The other areas of local measurements gave similar results and are not presented in Fig. 12.

The refractive index averaged over measured frequencies is virtually the same ($n = 2.4$) for all dentine sites and is considerably large for enamel ($n = 3.2$). The refractive index dispersion [9] only weakly varies in different tooth sites. The absorption spectrum can be approximated by the quadratic dependence $\alpha(f) = A + B_1 f + B_2 f^2$ (at least in the frequency range from 0.2 to 2.5 THz), where the coefficient at f^2 plays the main role (Fig. 12a). The averaged coefficients A, B_1, B_2 are 13, -21, and 36, respectively (f measured in THz and α in cm^{-1}). The refractive index can be assumed constant for most of the applications (Fig. 12b).

In spatial-resolution studies of different tooth regions (dentine, enamel, and intermediate area between them), the spatial resolution was increased by using a pinhole of diameter $D = 1$ mm placed on the sample surface on which radiation was focused. However, a broadband ($\lambda = 1000-100$ μm) THP can be focused only down to a spot of diameter 0.5–3 mm. For $D = 1$ mm, the THP intensity is reduced insignificantly, which retains the SNR $= 10^3$ necessary for reliable spectral measurements.

Considerable losses take place in the low-frequency part of the spectrum, where the wavelength is comparable with the aperture size. When D becomes smaller then λ, the signal amplitude decreases proportionally to D^4. Thus, to obtain the desirable spatial resolution of 100 μm, it is necessary to increase the SNR by an order of magnitude, which is still difficult to achieve in practice. The tissue image contrast in time-domain terahertz spectroscopy cannot be increased simply by using shorter wavelengths (higher terahertz frequencies) for two reasons. First, absorption in biological tissues considerably increases with frequency (Fig. 12) and, second, the efficiency of generation and detection of THPs considerably decreases at frequencies higher than 2–3 THz [8]. The reasonable optimal value of D providing the required spatial resolution and spectrum quality was 500 μm in our case in the frequency range from 0.3 to 2.5 THz.

4. Conclusions

The terahertz absorption spectra of some biological substances and tissues have been studied by using a terahertz spectrometer and methods developed for processing of measurements. Small organic molecules have characteristic absorption lines in the terahertz frequency range. Large molecules and tissues have considerable absorption, which almost linearly increases with frequency. The absorption coefficient and refractive index of liquid water determine the applicability of THPs (below 0.5 THz) for studying biological objects. Strongly absorbing substances can be studied by reflection spectroscopy. The terahertz spectra of a number of saccharides (glucose, fructose, saccharose, lactose, arabionse) and their solutions and mixtures have been measured in a new, broader frequency range from 0.3 to 3.5 THz. The absorption and refraction spectra of various tooth sites have been measured for the first time.

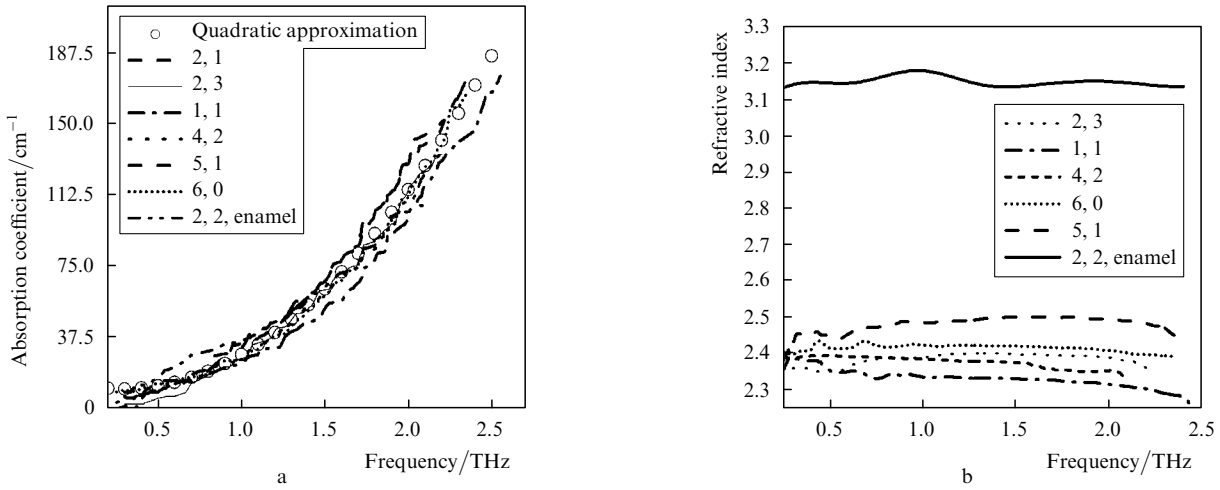

Figure 12. Absorption and refraction spectra of different tooth sites. The first and second numbers correspond to the sample number and site of measurements, respectively, in Fig. 11.

Acknowledgements. This work was supported by CRDF BRHE (Grant No. RUX0-006-SR-06), and the Russian Foundation for Basic Research (Grant No. 05-03-32877-a).

References

1. Brandt N.N., Chikishev A.Yu., Kargovsky A.V., Nazarov M.M., Parashchuk O.D., Sapozhnikov D.A., Smirnova I.N., Shkurinov A.P., Sumbatyan N.V. *Vibrational Spectroscopy*, **47**, 53 (2008).
2. Pickwell E., Cole B.E., Fitzgerald A.J., Pepper M., Wallace V.P. *Phys. Med. Biol.*, **49**, 1595 (2004).
3. Globus T., Woolard D., Crowe T.W., Khromova T., Gelmont B., Hesler J. *J. Phys. D: Appl. Phys.*, **39**, 3405 (2006).
4. Pickwell E., Wallace V.P. *J. Phys. D: Appl. Phys.*, **39**, R3010 (2006).
5. Fedorov V.I., Popova S.S. *Millimeter waves in biology and medicine*, **2**, 3 (2006).
6. Fitzgerald A.J., Berry E., Zinov'ev N.N., Homer-Vanniasinkam S., Miles R.E., Chamberlain J.M., Smith M.A. *J. Biol. Phys.*, **129**, 123 (2003).
7. Zhang X.-C., Hu B.B., Darrow J.T., Auston D.H. *Appl. Phys. Lett.*, **56**, 1011 (1990).
8. Nazarov M.M., Makarova S.A., Shkurinov A.P., Okhotnikov O.G. *Appl. Phys. Lett.*, **92**, 021114 (2008).
9. Nazarov M.M., Shkurinov A.P., Tuchin V.V. *Proc. SPIE Int. Soc. Opt. Eng.*, **6791**, 679109 (2008).
10. Nazarov M.M., Shkurinov A.P., Tuchin V.V., Zhernovaya O.S. *Proc. SPIE Int. Soc. Opt. Eng.*, **6535**, 65351J (2007).
11. Duvillaret L., Garet F., Coutaz J.-L. *J. Sel. Top. Quantum Electron.*, **2**, 739 (1996).
12. Withayachumnankul W., Ferguson B., Rainsford T., Mickan S.P., Abbott D. *Proc. SPIE Int. Soc. Opt. Eng.*, **5840**, 221 (2005).
13. Yamamota K., Kabir Md.H., Tominaga K. *J. Opt. Soc. Am. B*, **22**, 2417 (2005).
14. Brandt N.N., Chikishev A.Yu., Nazarov M.M., Okhotnikov O.G., Parashchuk O.D., Shkelnyuk S.A., Sapozhnikov D.A., Shkurinov A.P. *Proc. SPIE Int. Soc. Opt. Eng.*, **6194**, 619408 (2006).
15. Yamamoto K., Yamaguchi M., Myamaru F., Tani M., Hangyo M., Ikeda T., Matsushita A., Koide K., Tatsuno M., Minami Y. *Jpn. J. Appl. Phys.*, **43**, L414 (2004).
16. Dolotov L.E., Sinichkin Yu.P., Tuchin V.V., Utz S.R., Altshuler G.B., Yaroslavsky I.V. *Las. Surg. Med.*, **34**, 127 (2004).
17. Schaefer H., Redelmeier T.E. *Skin Barrier, Principles of Percutaneous Absorption* (Basel: Karger, 1996).
18. Tuchin V.V. *Tissue Optics: Light Scattering Methods and Instruments for Medical Diagnosis* (Bellingham, WA: SPIE Press, 2007, PM 166).
19. Crawley D.A., Lonbottom C., Wallace V.P., Cole B.E., Arnone D.D., Pepper M. *J. Biomed. Opt.*, **8**, 303 (2003).
20. Woods K.N., Wiedemann H. *J. Chem. Phys.*, **123**, 134507 (2005).
21. Wehrli F.W., Fernandez-Seara M.A. *Annal. Biomed. Eng.*, **33**, 79 (2005).
22. Kishen A., Rafique A. *J. Biomed. Opt.*, **11**, 054018 (2006).
23. Imbeni V., Nalla R.K., Bosi C., Kinney J.H., Ritchie R.O. *Inc. J. Biomed Mater. Res.*, **66A**, 1 (2003).